Obtaining the scattering rate of different T_{c0} FeSe thin films via spectroscopic ellipsometry

Yujun Shi, Jie Lian, Zhongpei Feng, Minglin Zhao, Kui Jin, Haonan Song, Mingyang Wei, Kai Dai, Qingfen Jiang, and Jiaxiong Fang

Citation: Journal of Vacuum Science & Technology B **37**, 052907 (2019); doi: 10.1116/1.5119394
View online: https://doi.org/10.1116/1.5119394
View Table of Contents: https://avs.scitation.org/toc/jvb/37/5
Published by the American Vacuum Society

Obtaining the scattering rate of different T_{c0} FeSe thin films via spectroscopic ellipsometry

Yujun Shi,[1] Jie Lian,[1,a)] Zhongpei Feng,[2] Minglin Zhao,[3] Kui Jin,[2] Haonan Song,[1] Mingyang Wei,[1] Kai Dai,[1] Qingfen Jiang,[1] and Jiaxiong Fang[4]
[1]*School of Information Science and Engineering, and Shandong Provincial Key Laboratory of Laser Technology and Application, Shandong University, Qingdao 266237, Shandong, China*
[2]*National Lab for Superconductivity, Institute of Physics, Chinese Academy of Sciences, Beijing 100190, China*
[3]*Department of Physics, Jiangsu University of Science and Technology, Zhenjiang 212003, Jiangsu, China*
[4]*Advanced Research Center for Optics, Shandong University, Jinan 250100, Shandong, China*

(Received 10 July 2019; accepted 4 September 2019; published 27 September 2019)

Due to the simplest crystalline structure among Fe-based superconductors, the FeSe system has attracted a lot of attention. In this work, FeSe thin films grown on the CaF_2 substrate with $T_{c0} = 6$ and 11 K (named FeSe_1 and FeSe_2, respectively) are fabricated by a pulsed laser deposition technique. X-ray diffraction exhibits a high-quality single crystal of the two FeSe samples, and the lattice constants are about 5.574 Å. Atomic force microscopy characterizes their surface topography and roughness, which shows stripes in their surfaces that is helpful to construct a roughness layer using the optical measurement spectroscopic ellipsometry (SE) technique. SE is a powerful tool to determine FeSe thin films' complex refractive index $N = n + ik$ and plasma oscillation frequency ω_p. These important parameters are related to scattering rate τ^{-1} for FeSe thin films. The results show that scattering rate τ^{-1} of FeSe_2 is significantly lower than that of FeSe_1 in the whole frequency testing range at room temperature, which may be the reason that FeSe_2 owns higher T_{c0} in low temperature than FeSe_1. *Published by the AVS.*
https://doi.org/10.1116/1.5119394

I. INTRODUCTION

High temperature superconductors (HTSs) are the perspective materials in the applications of lossless power transmission, magnetic levitation transport, and magnetic resonance imaging.[1] Since 2008, the discovery of the iron-based HTS has triggered much interest in these materials.[2,3] In particular, the PbO-type FeSe system owing to its simplest crystalline structure has been one of the most studied ones among iron-based HTSs; thus, FeSe provides a unique opportunity to research its structural, electromagnetic transport, and optical properties.[4–7] Among these properties, a blank space to research FeSe optical constants remains, which can help researchers to learn more about FeSe.

As we know, complex optical constants $N = n + ik$ (n is the refractive index and k is the extinction coefficient) or complex dielectric functions $\varepsilon = \varepsilon_r + i\varepsilon_i$ (ε_r and ε_i are the real part and the imaginary part of ε, respectively) contain rich physical information. Because optical constants can not only characterize energy band transition for kinds of materials, for instance, two-dimensional (2D) MoS_2,[8] perovskite $CsPbBe_3$[9] material and spinel oxide $MgTi_2O_4$ (Ref. 10), etc., also are related with electrical quantities, such as scattering rate τ1 and complex optical conductivity $\sigma = \sigma_1 + i\sigma_2$ (σ_1 and σ_2 are the real part and the imaginary part of σ, respectively). Compared with reflectivity, SE measures the amplitude and phase information simultaneously and need not use Kramers–Kronig (K–K) transformation in a broad frequency testing range. Therefore, SE has become a suitable and convenient method to determine N or ε.

As mentioned above, N or ε is associated with scattering rate τ^{-1} and complex optical conductivity σ, which are important parameters to analyze the intrinsic nature of FeSe. For example, Chinotti *et al.* provided that the interplay of the anisotropic scattering rate and Drude weight results in the nematic phase in the low energy excitation spectrum in the FeSe system.[14] Yuan *et al.* measured the in-plane optical conductivity σ_1 of FeSe thin films and found two Drude components existing in the low-frequency optical conductivity σ_1 spectrum.[5] Actually, it is worth noting that the plasma oscillation frequency ω_p plays an important role in obtaining the scattering rate. In previous works, ω_p is usually calculated by an integral form, whereas the upper limit of the integral is hard to decide.[15] However, significant advantage exsits in SE method for obtaining ω_p because Drude dispersion law encompasses this parameter in fitting measurement data process.

Therefore, in this work, SE is employed to obtain complex refractive index N for two FeSe thin films with superconducting transition temperature $T_{c0} = 6$ and 11 K that are named FeSe_1 and FeSe_2, respectively. Drude and Lorentz oscillation dispersion laws are used to invert the SE measurement data tan Ψ and cos Δ, and ω_p is derived using the Drude model. Finally, scattering rate τ^{-1} is calculated through σ for FeSe_1 and FeSe_2, which may provide some information about the phenomenon in low temperature.

Note: This paper is part of the Conference Collection: 8th International Conference on Spectroscopic Ellipsometry 2019, ICSE.
a)Electronic mail: jieliansdu@163.com

II. EXPERIMENT

There are two FeSe thin films with $T_{c0} = 6$ and 11 K grown on CaF_2 substrates in this work, and they were deposited by the pulsed laser deposition (PLD) technique in a vacuum chamber. The details (synthesis and electrical measurement) of FeSe samples have been documented elsewhere.[6] Crystallinity is characterized by x-ray diffraction (XRD, D8ADVANCE) with an x-ray wavelength of $\lambda = 1.54$ Å. Surface topography and roughness are measured by atomic force microscopy (AFM, Nanosurf). SE (GES-5, SOPRA) with a rotating analyzer is utilized to determine the complex optical constants of FeSe thin films, and the software WINELLI supplied by SOPRA is used to data analysis. To get smoother ellipsometric data, the spectral resolution is set to 5 nm in 300–800 nm wavelength (energy ranges from 1.55 to 4.13 eV and frequency from 12 500 to 33 333 cm^{-1}). The incident angle is fixed at 75°, which is close to Brewster angle and the testing condition is room temperature.

A. Crystal structure

As mentioned above, PbO-type FeSe has the simplest lattice structure in Fe-based superconductors that the FeSe unit consists of three layers with the central Fe layer sandwiched in between two adjacent Se layers,[7] as shown in the inset of Fig. 1. The lattice diffraction patterns of FeSe_1 and FeSe_2 thin films grown on the CaF_2 substrate are exhibited in Fig. 1 by XRD. The two samples' diffraction peaks show an orientation along (00l), which demonstrates that FeSe thin films are fabricated with a high-quality single crystal. The c-axis lattice constant is calculated from the XRD results using the Bragg law,

$$2 \cdot d \cdot \sin\theta = n \cdot \lambda, \tag{1}$$

where θ is the diffraction angle and n is the order of reflection. FeSe_1 and FeSe_2 exhibit similar values of the c-axis lattice parameter that is 5.574 Å, which is very close to the result of 5.8 Å reported by Feng *et al.*[6] The high-quality samples open a credible door for the investigation of optical measurement and physical discussion.

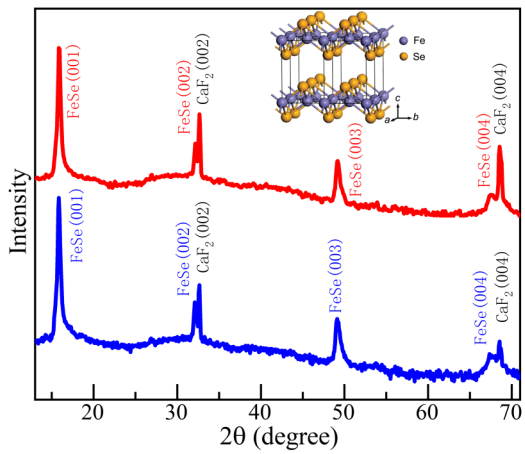

FIG. 1. XRD patterns of FeSe_1 (upper line) and FeSe_2 (lower line) grown on CaF_2 substrates, and the diffraction peaks of CaF_2 are indicated in black words. The inset is the unit cell of FeSe.

B. Surface topography

AFM is not only a versatile tool to obtain abundant information on surfaces, but also a useful approach to get roughness data for removing this roughness layer to optical constants in SE analysis. Figure 2 is the surface condition of FeSe thin films. In the $2 \times 2\,\mu m^2$ test range, homogenous light stripes are observed in the surface. The width of these stripes is about 208.5 and 260.1 nm for FeSe_1 and 2 samples that are illustrated using the pink arrows between double green lines in Figs. 2(b) and 2(e), respectively. The cross-section information is shown in Figs. 2(c) and 2(f), which can justifiably offer the visual roughness layer in building an optical structure, and this will be discussed in Sec. II C. Here, we do not focus the question on how these light stripes are formed, just put the point to SE analysis.

C. SE data analysis

1. Ellipsometry and experiment

As a nondestructive and accurate optical technique, tan Ψ and cos Δ are the direct measurement values by SE, which are related to the amplitude ratio and phase difference between p- and s-polarizations, defined by the following equation:

$$\rho \equiv \tan(\Psi)\exp(i\Delta) \equiv \frac{r_p}{r_s}, \tag{2}$$

where r_p and r_s express Fresnel coefficients for p- and s-polarized light, respectively. The Fresnel coefficients depend on the complex optical constants $N = n + ik$ and the thin film thickness.[16] However, Eq. (2) is a nonlinear transcendental equation, and there is no possibility to directly obtain the analytic solutions.[17] Generally, to achieve the complex optical constants by SE, one should construct the optical structure model that includes substrate, interface, film, and/or roughness layers information, etc., and film thickness to fit tan Ψ and cos Δ. Specially, one should emphatically take considering to the appropriate dispersion law and suitable free parameters for the layer of thin film that is measured because it is a crucial step to inverse measurement data.

2. Model construction

With the accurate and precision measurement values of tan Ψ and cos Δ, a suitable model including the optical model and the dispersion model should be constructed. First, to remove the effect of roughness on the complex optical constants or dielectric functions, the roughness layer should be added in the optical model. Thus, a four-phase optical model is used to describe the FeSe_1 and FeSe_2 film system, that is the void/roughness layer/FeSe layer/CaF_2 substrate. Based on AFM, the homogeneous triangle microstructure has been determined for FeSe_1; thus, the roughness

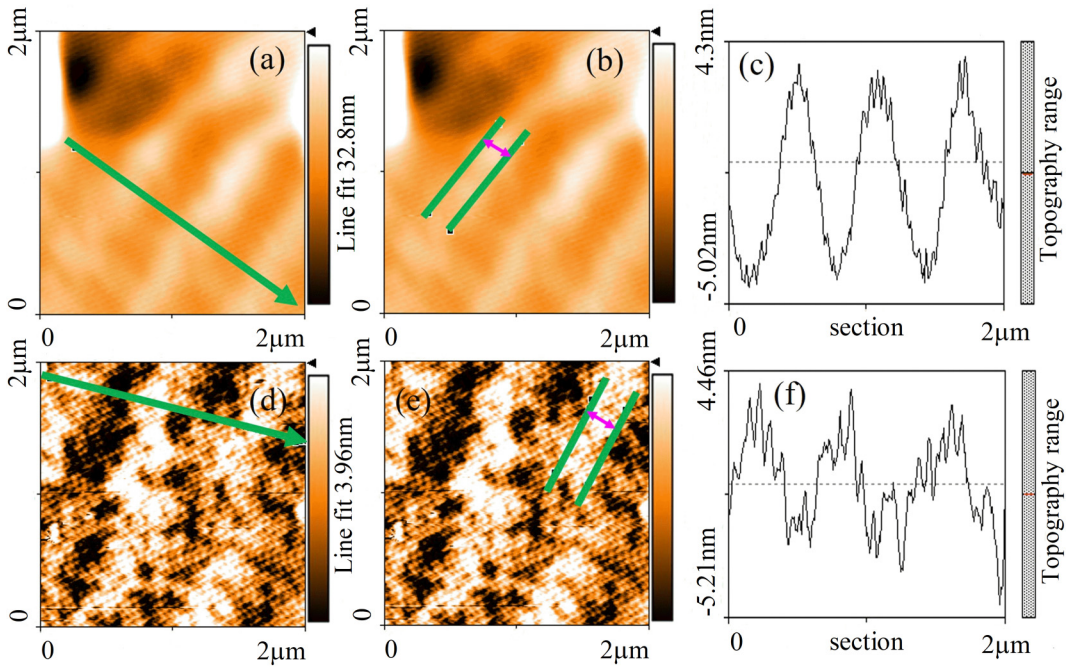

FIG. 2. AFM surface characterization of (a) for FeSe_1 and (d) for FeSe_2. (b) and (e) illustrate the width of the light stripes, and (c) and (f) are the cross-section topography for the green arrows in (a) and (d) for FeSe_1 and FeSe_2 sample, respectively.

layer consisted of 50% void and 50% FeSe described by the Bruggeman effective-medium approximation, and then, we fixed the concentration during the fitting process. In addition, the root mean square roughness is 5.44 nm by AFM and is 5.72 nm by SE, demonstrating that the roughness obtained by AFM can provide indicative information about SE data analysis. However, for FeSe_2, there are more burrs in the cross-section. Therefore, a good fitting result is 18% void

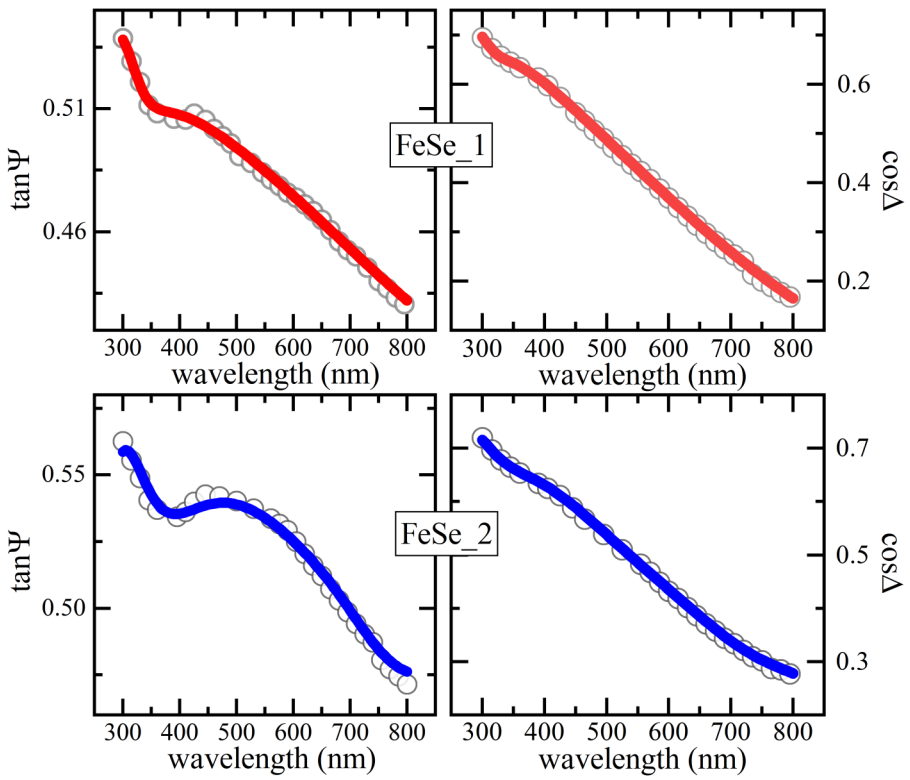

FIG. 3. Experimental data (marked by hollow circle) and simulated data (red lines for FeSe_1 and blue lines FeSe_2) of tan Ψ and cos Δ.

TABLE I. Fitting parameters' value for the FeSe_1 sample.

Drude				Lorentz		
P	ω_p (μm^{-1})	τ^{-1} (μm^{-1})		A	L_0 (μm)	γ (μm)
0.626 ± 0.089	12.611 ± 0.179	15.185 ± 0.216	Peak1	2.187 ± 0.311	0.832 ± 0.012	0.813 ± 0.016
			Peak2	0.541 ± 0.007	0.220 ± 0.003	0.001 ± 0.001
			Peak3	0.165 ± 0.002	0.323 ± 0.004	0.101 ± 0.001

and 82% FeSe_2 for the mixing concentration, and the thickness of roughness is 18.2 nm by SE, which is higher than that of 7.1 nm by AFM.

Then, Drude, describing the free electrons in metals, and Lorentz dispersion laws are chosen to fit tan Ψ and cos Δ since FeSe is a superconductor in low temperature. A consistent fitting result between experimental and simulated data has been obtained, as shown in Fig. 3. Here, we simply introduce Drude and Lorentz dispersion law functions,

$$\text{Drude:}\begin{cases}\varepsilon_r = P - {\omega_p}^2{*}\lambda^2/[1+(\lambda{*}\tau^{-1})^2],\\ \varepsilon_i = \tau^{-1}{*}{\omega_p}^2{*}\lambda^3/[1+(\lambda{*}\tau^{-1})^2],\end{cases} \tag{3}$$

$$\text{Lorentz:}\begin{cases}\varepsilon_r = A{*}\lambda^2{*}(\lambda^2-{L_0}^2)/[(\lambda^2-{L_0}^2)^2+\gamma^2{*}\lambda^2],\\ \varepsilon_i = A{*}\lambda^3{*}\gamma/[(\lambda^2-{L_0}^2)^2+\gamma^2{*}\lambda^2],\end{cases} \tag{4}$$

where P is the polarization, ω_p is the plasma oscillation frequency, and τ^{-1} is the scattering rate of free electrons for the Drude model. For the Lorentz oscillator, A is the intensity, L_0 is the central wavelength, and γ is the width of the peak. Tables I and II list the best fitting parameters' value for FeSe_1 and 2, respectively. The complex refractive index can be solved from the dielectric functions according to the following equations:[18,19]

$$n = \left\{\frac{[\varepsilon_1 + ({\varepsilon_1}^2+{\varepsilon_2}^2)^{1/2}]}{2}\right\}^{1/2}, \tag{5}$$

$$k = \left\{\frac{-\varepsilon_1 + ({\varepsilon_1}^2+{\varepsilon_2}^2)^{1/2}}{2}\right\}^{1/2}. \tag{6}$$

3. Ellipsometry data analysis

After establishing the above optical model and dielectric functions, the theoretical results of tan Ψ and cos Δ for FeSe thin films can be calculated by a regression method.[18] To evaluate the goodness of the fitting parameters between experimental results and theoretical calculation, the mean squared error (*MSE*) is defined by the following function, which relative small values are exhibited in Table III,

$$MSE = \frac{1}{2n-m-1}\sum_{i=1}^{n}\left[(\tan\Psi^i_{cal}-\tan\Psi^i_{exp})^2 + (\cos\Delta^i_{cal}-\cos\Delta^i_{exp})^2\right], \tag{7}$$

where n is the number of tan Ψ and cos Δ, m is the number of fitting parameters, and the subscripts *cal* and *exp* represent the theoretical calculation results and experimental results, respectively.

As we know, the dispersion law is an efficient method to invert the measurement data tan Ψ and cos Δ. However, point-by-point is also a resultful way to generate refractive index n and extinction coefficient k.[17,20,21] Figure 4 is the n and k comparative results for the two FeSe samples by the methods of dispersion law marked by solid lines and point-by-point illustrated by gray lines. Very consistent consequences of n and k are obtained by the two means, indicating the validity of the Drude and Lorentz dispersion law and fitting parameters.

III. RESULTS AND DISCUSSION

To understand why FeSe owns different T_{c0} at low temperature, the scattering rate of free electrons τ^{-1} at room temperature may provide some information. τ^{-1} is related to optical conductivity $\sigma(\omega)$, whereas $\sigma(\omega)$ can be achieved by complex refractive index $N = n(\omega) + ik(\omega)$ or dielectric functions $\varepsilon = \varepsilon_r(\omega) + i\varepsilon_i(\omega)$. The equations are shown as follows:[11]

$$\tau^{-1}(\omega) = \frac{{\omega_p}^2}{4\pi}\frac{\sigma_1(\omega)}{{\sigma_1}^2(\omega)+{\sigma_2}^2(\omega)}, \tag{8}$$

$$\sigma_1(\omega) = \frac{\omega[\varepsilon_i(\omega)+1]}{4\pi} = \frac{\omega[2n(\omega)k(\omega)+1]}{4\pi}, \tag{9}$$

TABLE II. Fitting parameters' value for FeSe_2 sample.

Drude				Lorentz		
P	ω_p (μm^{-1})	τ^{-1} (μm^{-1})		A	L_0 (μm)	γ (μm)
0.171 ± 0. 002	7.521 ± 0.107	4.524 ± 0.064	Peak1	0.688 ± 0.009	0.329 ± 0.005	0.140 ± 0.002
			Peak2	0.224 ± 0.003	0.715 ± 0.012	0.220 ± 0.003
			Peak3	0.746 ± 0.011	0.256 ± 0.003	0.009 ± 0.001

TABLE III. *MSE* results for FeSe_1 and FeSe_2.

	FeSe_1	FeSe_2
MSE (10^{-4})	3.298	3.131

$$\sigma_2(\omega) = -\frac{\omega\varepsilon_r(\omega)}{4\pi} = \frac{\omega[k^2(\omega) - n^2(\omega)]}{4\pi}, \tag{10}$$

where ω_p is the plasma oscillation frequency which has been obtained by the Drude dispersion law in the fitting process in Eq. (8) and ω is the frequency.

Owing to the fact that $N = n(\omega) + ik(\omega)$ or $\varepsilon = \varepsilon_r(\omega) + i\varepsilon_i(\omega)$ have been characterized by SE, the optical conductivity $\sigma(\omega)$ is easy to be obtained. ω_p is derived by the Drude dispersion law, which are 12.611 and 7.521 μm^{-1} for FeSe_1 and FeSe_2, respectively. These values are similar to the 10.9 μm^{-1} characterized by optical reflectance $R(\omega)$ at room temperature on FeSe thin films grown on the $SrTiO_3$ substrate by Yuan *et al.*[5] Then, we substitute $\sigma(\omega)$ and ω_p into Eq. (8) and τ^{-1} could be obtained, which are illustrated in Fig. 5. After normalization, it is intuitive to conclude that τ^{-1} of FeSe_2 is obviously lower than that of FeSe_1 in the whole measurement frequency, which demonstrates that the metallicity of FeSe_2 is obviously better than FeSe_1. Therefore, we conclude that the higher T_{c0} in the FeSe_2 sample with 11 K maybe originated from the lower scattering rate compared with FeSe_1 with 6 K at room temperature.

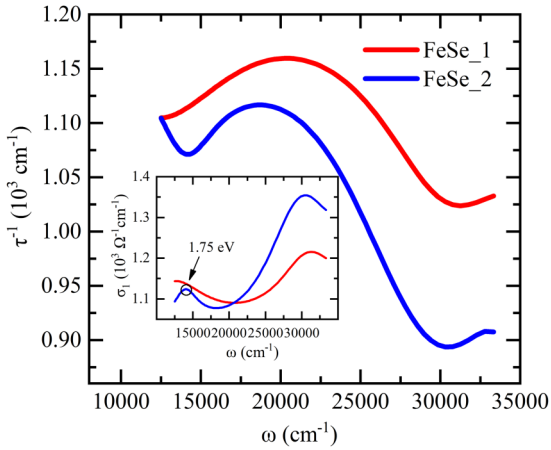

FIG. 5. Scattering rate of free electrons τ^{-1} depends on the frequency ω at room temperature for FeSe_1 (red line) and FeSe_2 (blue line). The inset is the real part of optical conductivity $\sigma_1(\omega)$ and the arrow indicates a 1.75 eV peak existing in the FeSe_2 sample.

The real part of optical conductivity $\sigma_1(\omega)$ is also shown in the inset of Fig. 5, the trend of frequency-dependent behavior is similar to the work of Wen *et al.*,[22] as well as the FeSe counterpart Fe-pnictogen compounds.[23,24] It is worth noting that the peak at about 1.75 eV in FeSe_2 can be attributed to the transition from Fe *d* level to Fe-d/Se-p hybridized orbitals, corresponding to the two major peaks of the density of states near E_F.[25] However, this transition has not been observed in FeSe_1, and the reason will be discussed in further.

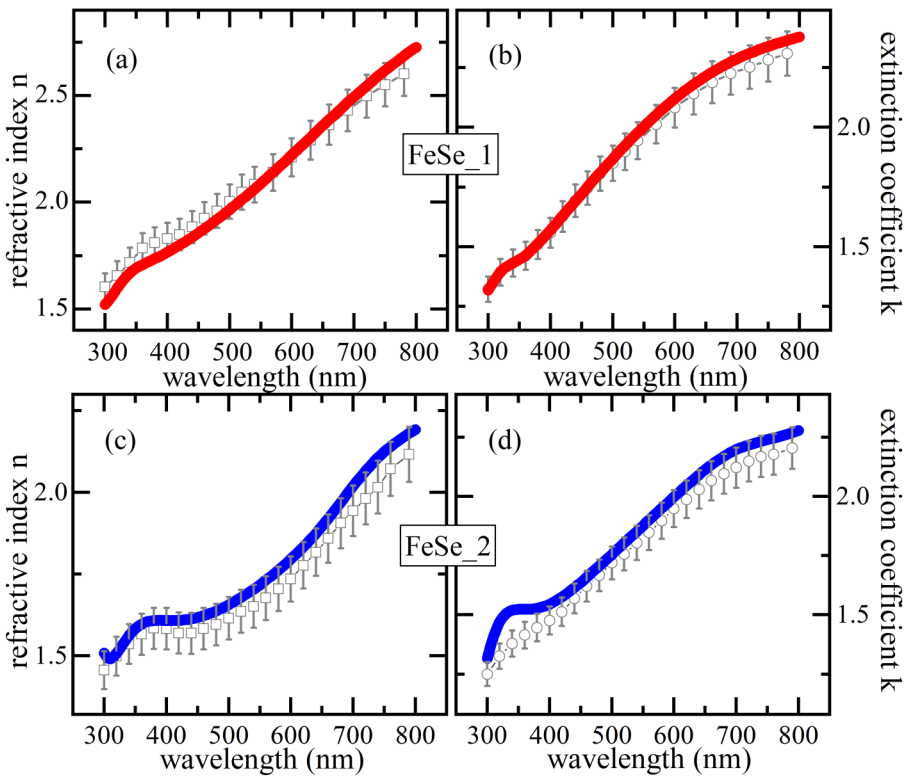

FIG. 4. Comparative results by the methods of dispersion law (solid lines) and point-by-point (gray lines). (a) and (b) are refractive index *n* and extinction coefficient *k* for FeSe_1, and (c) and (d) are *n* and *k* for the FeSe_2 sample.

IV. SUMMARY AND CONCLUSIONS

FeSe thin films with different T_{c0} fabricated by the PLD technique exhibit a high-quality single crystal measured by XRD and the lattice constant is about 5.574 Å. The surface topography characterized by AFM shows that light stripes exist in FeSe thin films. It is helpful to construct an optical structure model in SE data analysis and offer the thickness of roughness. Using the Drude and Lorentz dispersion laws to fit $\tan\Psi$ and $\cos\Delta$, complex refractive index N or dielectric functions ε are derived from calculating scattering rate τ^{-1}. The result turns out that τ^{-1} of FeSe_2 with 11 K transition temperature is significantly lower than that of FeSe_1 with $T_{c0} = 6$ K at room temperature, which may be the reason that FeSe_2 exhibits higher T_{c0} in low temperature than FeSe_1. Therefore, we provide a feasible way to relate optical constants with electric quantities for the FeSe system.

ACKNOWLEDGMENTS

This work was funded by the grants from the National Key Basic Research Program of China (No. 2015CB921003), the Key Research and Development Project of Shandong Province (No. 2017GGX201008), and the National Natural Science Foundation of China (No. 11804126).

[1]M. Y. Qin, Z. F. Lin, Z. X. Wei, B. Y. Zhu, J. Yuan, I. Takeuchi, and K. Jin, Chin. Phys. B **27**, 127402 (2018).
[2]Y. Kamihara, T. Watanabe, M. Hirano, and H. Hosono, J. Am. Chem. Soc. **130**, 3296 (2008).
[3]F. C. Hsu *et al.*, Proc. Natl. Acad. Sci. U.S.A. **105**, 14262 (2008).
[4]Q. Y. Wang *et al.*, Chin. Phys. Lett. **29**, 037402 (2012).
[5]R. H. Yuan, W. D. Kong, L. Yan, H. Ding, and N. L. Wang, Phys. Rev. B **87**, 144517 (2013).
[6]Z. P. Feng *et al.*, Sci. Rep. **8**, 4039 (2018).
[7]X. Liu *et al.*, J. Phys. Condens. Matter **27**, 183201 (2015).
[8]B. K. Song, H. G. Gu, M. S. Fang, X. G. Chen, H. Jiang, R. Y. Wang, T. Y. Zhai, Y. T. Ho, and S. Y. Liu, Adv. Opt. Mater. **7**, 1801250 (2019).
[9]M. L. Zhao, Y. J. Shi, J. Dai, and J. Lian, J. Mater. Chem. C **6**, 1 (2018).
[10]Y. J. Shi, J. Lian, W. Hu, Y. X. Liu, G. He, K. Jin, H. N. Song, K. Dai, and J. X. Fang, J. Alloys Compd. **788**, 891 (2019).
[11]A. Charnukha, J. Phys. Condens. Matter **26**, 253203 (2014).
[12]Y. J. Jiang, A. M. Soufiani, A. Gentle, F. Z. Huang, A. Ho-Baillie, and M. A. Green, Appl. Phys. Lett. **108**, 061905 (2016).
[13]Y. M. Zhang *et al.*, IEEE Photonics J. **11**, 1 (2019).
[14]M. Chinotti, A. Pal, L. Degiorgi, A. E. Böhmer, and P. C. Canfield, Phys. Rev. B **98** (2018).
[15]H. P. Wang, Z. R. Ye, Y. Zhang, and N. L. Wang, Sci. Bull. **61**, 1126 (2016).
[16]H. Fujiwara, *Spectroscopic Ellipsometry Principles and Applications* (Maruzen, Tokyo, 2007).
[17]Z. Z. Sun, J. Lian, S. Gao, X. Wang, Y. S. Wang, and X. H. Yu, J. Comput. Theor. Nanosci. **11**, 816 (2014).
[18]B. K. Song, H. G. Gu, S. M. Zhu, H. Jiang, X. G. Chen, C. W. Zhang, and S. Y. Liu, Appl. Surf. Sci. **439**, 1079 (2018).
[19]Y. X. Liu, J. Lian, M. L. Zhao, Y. Wang, M. M. Li, and H. N. Song, Europhys. Lett. **117**, 57007 (2017).
[20]M. L. Zhao, J. Lian, Z. Z. Sun, W. F. Zhang, M. M. Li, Y. Wang, H. S. Yu, K. Jin, and X. Y. Hu, Opt. Mater. Express **5**, 2047 (2015).
[21]M. L. Zhao, J. Lian, Z. Z. Sun, X. Wang, W. F. Zhang, J. J. Hu, and M. M. Li, Mod. Phys. Lett. B **28**, 1450196 (2014).
[22]Y. C. Wen, K. J. Wang, H. H. Chang, J. Y. Luo, C. C. Shen, H. L. Liu, C. K. Sun, M. J. Wang, and M. K. Wu, Phys. Rev. Lett. **108**, 267002 (2012).
[23]A. Charnukha, P. Popovich, Y. Matiks, D. L. Sun, C. T. Lin, A. N. Yaresko, B. Keimer, and A. V. Boris, Nat. Commun. **2**, 219 (2011).
[24]A. Charnukha, D. Pröpper, T. I. Larkin, D. L. Sun, Z. W. Li, C. T. Lin, T. Wolf, B. Keimer, and A. V. Boris, Phys. Rev. B **88**, 184511 (2013).
[25]A. Subedi, L. Zhang, D. J. Singh, and M. H. Du, Phys. Rev. B **78**, 134514 (2008).